NUKLEONIKA 2006;51(1):71–78

Surface and bulk processes in materials induced by pulsed ion and plasma beams at Dense Plasma Focus devices

**Valeriy N. Pimenov,
Sergey A. Maslyaev,
Lev I. Ivanov,
Elena V. Dyomina,
Vladimir A. Gribkov,
Alexander V. Dubrovsky,
Marek Scholz,
Ryszard Miklaszewski,
Ülo E. Ugaste,
Blagoslav Kolman**

Abstract A review of results and new data on the interaction of pulsed ion and dense plasma beams with metals in different Dense Plasma Focus (DPF) devices are presented. Different irradiation conditions with microsecond pulses of the power density in the range of 10^5–10^9 W/cm^2 were applied. The most interesting thermal and radiation effects observed in both surface and bulk of the material positioned at the cathode part of the DPF device have been considered. Advanced directions of DPF use for scientific and applied problems of radiation material science were determined.

Key words Plasma Focus • pulse irradiation • surface damage

V. N. Pimenov✉, S. A. Maslyaev, L. I. Ivanov,
E. V. Dyomina, V. A. Gribkov
A. A. Baikov Institute of Metallurgy
and Material Science, Russian Academy of Sciences,
49 Leninsky Pr., 119991 Moscow, Russia,
Tel.: +7 095 135 9604, Fax: +7 095 135 8680,
E-mail: pimval@mail.ru

A. V. Dubrovsky
Moscow Physical Society,
53 Leninsky Pr., 117924 Moscow, Russia

M. Scholz, R. Miklaszewski
Institute of Plasma Physics and Laser Microfusion,
23 Hery Str., 00-908 Warsaw, P. O. Box 49, Poland

Ü. E. Ugaste
Tallinn Pedagogical University,
25 Narva Road, 10120 Tallinn, Estonia

B. Kolman
Institute of Plasma Physics ASCR,
3 Za Slovankou Str., P. O. Box 17, 18221 Prague 8,
Czech Republic

Received: 25 August 2005
Accepted: 8 November 2005

Introduction

Dense Plasma Focus (DPF) devices, unlike other thermonuclear devices, have a number of important advantages.

1) They provide an opportunity to expose materials to pulsed beams of various types (ion, electron, plasma, X-ray, neutron and shock wave) of high-power flux density (up to 10^{14} W/cm^2) with pulse duration in the range from 10^{-8} to 10^{-6} s.
2) They ensure an opportunity to vary the distribution of pulse energy between ion and plasma beams: energy flux density of ion and plasma beams may be significantly different depending on the mode of irradiation.
3) These beams in DPF devices can be separated in the time due to the different velocity (within one order of magnitude) [2, 23] of ion beam and plasma jet. The problem of plasma-surface interaction is especially amenable to the study of damage to materials under high-power energy pulses generated in different radiation devices including DPF devices, chambers for inertial (laser and heavy ion fusion) and magnetic (TOKAMAK and stellarator) confinement thermonuclear fusion.

During the last few years, we performed investigations on material damage under pulsed ion and high temperature plasma (HTP) beams in different PF devices in the frame of national and international scientific programmes. Obtained results showed that the influence of pulsed high-energy ($E_i \geq 100$ keV) ion beams and HTP (particle velocity $\sim 5 \times 10^7$ cm/s) on the target material results in a remarkable distinction in radiation and thermal effects in dependence of irradi-

ation conditions. The features of physical and chemical processes, structure-phase transformations and elements distribution in irradiated materials are different, too. All of that lead to the different material damage and change of its properties and chemical content.

The present paper deals with the most interesting results obtained within these investigations on the basis of international co-operation (particularly in the frame of INCO COPERNICUS research contract IC-15-CT98-0811 and the project of the International Atomic Energy Agency "Dense Magnetized Plasma"). Most results were previously published in the papers [2, 5–7, 9–11, 18–24, 26]. In addition, the data of new experiments and investigations, which were carried out recently, are presented. On the basis of the analysis and generalization of obtained results, the estimation of the prospects of PF device application for scientific and applied problems of radiation material science is made.

Materials

The following materials were chosen for the experiments: austenitic chromium-manganese and ferritic steels, pure vanadium, tungsten, graphite, copper, aluminum and their alloys, as well as sapphire [2, 6, 10, 18–20]. These metals and optic materials have a great potential to be applied in structural and functional components of thermonuclear fusion devices with magnetic [4] and inertial [14] plasma confinement, as well as for working chambers of plasma devices [2, 3, 5]. This paper presents only results for some materials, namely austenitic and ferritic steels and a copper-aluminum alloy. Specimens were prepared, as a rule, as plates of dimension $1.5 \times 0.5 \times 0.1$ cm^3. In special experiments, the specimen-target had a specific configuration: it was made in the form of a cylindrical tube and was placed along the axis of the working chamber of the plasma focus device PF-1000 [23, 24] (see Fig. 5). The outer diameter of the tube was 3 cm, the thickness of the tube wall $h = 0.25$ cm, the length of the tube $L = 24$ cm. A special screen of an aluminum alloy (5 cm in diameter) was placed on the end of the tube anode side in order to decrease the power flux density and to protect the inner surface of the tube from any kind of irradiation except the neutron stream. The screen protected the outer surface of the tube from direct influence of high-energy ions ($E \geq 100$ keV) and X-rays.

Experiment

The experiments were carried out by using two different types of DPF devices: PF-60, which has a Filippov-type (plane) electrode geometry [2, 3, 18] with deuterium as working gas (initial pressure of about 40 Pa); PF-1000 (see Fig. 5) and PF-6, which have a Mather-type (cylindrical) electrode geometry [2, 5, 10, 13, 19–24], with deuterium or hydrogen as working gases (~400 Pa). Samples of materials were positioned at the cathode part of the devices. In the experiments, we used for the irradiation plasma jets and beams of fast ions in a broad range of power flux densities. Influence of other types of radiation was negligible in these experiments. Pulsed irradiation of specimens was performed in different regimes: by microsecond high-temperature plasma pulses with power flux density $q = 10^7$–10^9 W/cm^2 (PF-1000, PF-6), and by 100-nanosecond deuterium plasma (DP) pulses with $q = 10^5$–10^{10} W/cm^2 (PF-60). In each shot in the PF-60 device a specimen was irradiated with a powerful high-energy ion pulse ($E_i \geq 100$ keV) and then, about 1 microsecond later, with the plasma jet. The energies of these two streams were approximately the same. In the case of the PF-1000 device ion and plasma beams in some experiments were separated in time and made a different energy contribution to the target material damage [19–21]. As it was shown in [21], the fast ion beam, having a very low energy content ($q < 1$ W/cm^2), hit the target about 6–8 μs earlier than the plasma jet, whereas the latter contributed the main part of the energy to the surface damage.

Ion implantation

Low-activation austenitic and ferritic steals are of major interest because they do not give long-lived isotopes under neutron irradiation [1, 9, 12, 15, 16, 27]. One aim of our previous works was to determine DPF operation modes with a low power flux density, which would be favourable for deuterium ion implantation into the material to form an implanted near-surface layer, and contrary to find regimes, which would prevent from the above-mentioned process. Under different power densities, three typical regimes of the influence of ion and plasma beam upon the target material were found.

1. It was shown that in the absence of the fast ion beam and at an irradiation power flux density of about 10^5–10^7 W/cm^2, the 'implantation mode' was realised. High concentration (more than 12 at.%) of deuterium in the target can be reached (see Fig. 1).

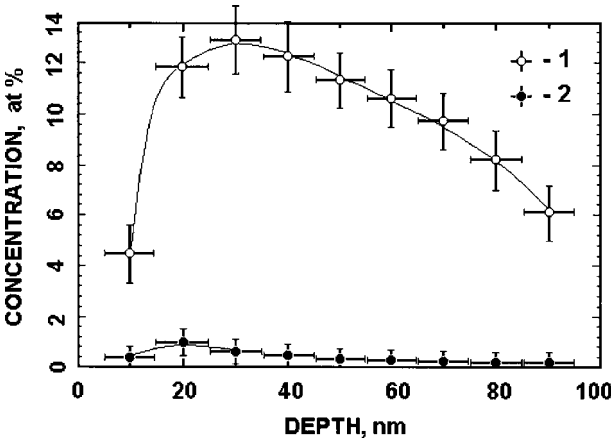

Fig. 1. Deuterium concentration distribution in the surface layer of austenitic chromium-manganese 25Cr12Mn20W steel after irradiation with 120 low power flux density plasma pulses: 1 – in the centre of irradiated region; 2 – point closed to the border of irradiated region ($q = 10^5$–10^7 W/cm^2).

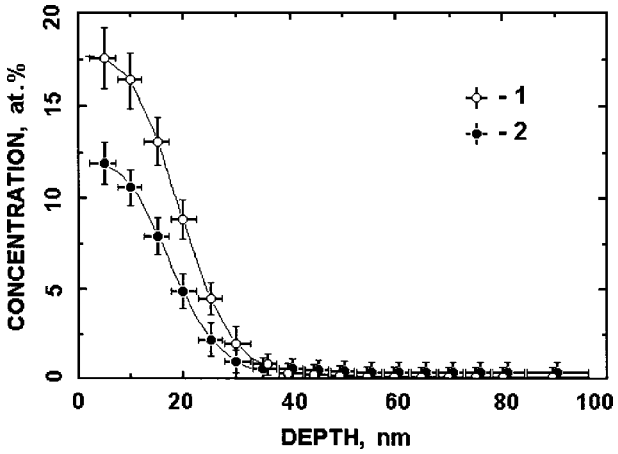

Fig. 2. Deuterium concentration distribution in the surface layer of ferritic 10Cr9W steel after irradiation with 5 medium power flux density pulses of plasma jet and beam of fast ions: 1 – in the centre of irradiated region; 2 – in the periphery of irradiated region (q = 10^7–10^8 W/cm^2).

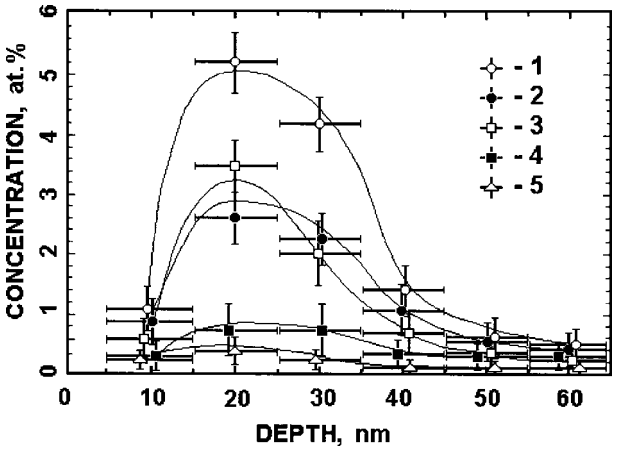

Fig. 3. Deuterium concentration distribution in the surface layer of austenitic chromium-manganese 25Cr12Mn20W steel after multifold irradiation with pulses of high power flux density plasma jet and fast ion beam: 1 – pulse; 2 – 2 pulses; 3 – 4 pulses; 4 – 8 pulses; 5 – 16 pulses (q = 10^9–10^{10} W/cm^2).

The implanted ion concentration increases with the number of pulses. Concentration distribution is governed by the diffusion process. It was also shown that in this regime of irradiation ($q \sim 10^6$ W/cm^2, pulse duration $\tau \sim 1$ μs) the surface layers of all tested materials were melting.

2. If the irradiation power flux density was increased to 10^7–10^8 W/cm^2, the 'detachment effect' rules the interaction process. The cloud of the plasma in front of the specimen's surface is produced mainly by the beam of fast ions which penetrates the material surface up to the order of the ion projective range (~0.5 μm) and evaporates it. The plasma of the jet and of its shock wave with low energy ions cannot reach the specimen's surface resulting in the formation of a very thin surface implantation layer of deuterium. At the medium power flux density q = 10^7–10^8 W/cm^2 (Fig. 2), we have also rather a high concentration of deuterium, but at the surface of the specimen (up to only 30 nm).
3. It has been found that when the power flux density increases up to 10^9–10^{10} W/cm^2 the so-called broken implantation ("explosive rupture" implantation) is observed. At this regime, a surface layer implanted by 1 irradiation pulse of about 100 keV deuterons appears to be completely evaporated, while the concentration of the implanted low energy deuterons ($E_i \sim 1$ keV) in the specimen decreases with the number of irradiation pulses (Fig. 3). This last feature finds its explanation on the basis of the successive diffusion enhancement due to the evolution of the topographical structure of the irradiated surface and because of the influence of the shock wave, generated inside the bulk of the material due to its ablation [7].

The presented results show the problem, which exists in technological application of PF device for implantation of working gas ions into material. It is connected with the melting of the surface layer of most materials under heat load $q \geq 10^6$ W/cm^2 and pulse duration $\tau \approx 0.1$–1 μs. To avoid this effect, the power density q should be in the range of 10^3–10^6 W/cm^2 depending on the melt temperature of the material. However, the time required for the formation of a uniformly implanted layer of sufficient thickness may be rather long. The solution to this problem may be connected with the use of high frequency (~10 Hz) PF devices with low energy (≤ 10 kJ).

Redistribution of elements

As it was noted above, the PF-1000 device allows realising the special regime of irradiation: the ion and plasma components of the energy pulse are separated temporary and make different energy contribution to the material damage.

In the works [19–21], the austenitic chromium-manganese 25Cr12Mn20W and 10Cr12Mn20W steels were irradiated in the described regime. The distribution of the elements before and after irradiation was analyzed qualitatively. The distributions of Fe, Mn and Cr in the initial state of the steel specimens were uniform. But after 3 pulses of irradiation a redistribution of the components on the surface of 10Cr12Mn20W steel was observed (see Fig. 4). In areas where radiation defects blisters-type occurred, a remarkable increase of the Mn content and a reduction of the Fe content took place. After 6 pulses this effect remained but was less evident. Where radiation induced craters (in both types of austenitic steels), a significant increase (~ 3–5 times as much [19, 20]) of the carbon and the oxygen content was observed.

We suppose [19, 21] that the implanted hydrogen ions have created vacancy clusters [28, 29]. This cluster appears to act as a nucleus of gas phase (micropore) and hence a sink for atoms of the light elements. Under the subsequent (6–8 μs later) heating by the plasma jet, Mn, as well as compounds of light elements CO, CO_2 may be collected in these micropores, with the formation and growth of gas bubbles. After crystallization and cooling, these bubbles (blisters) burst with

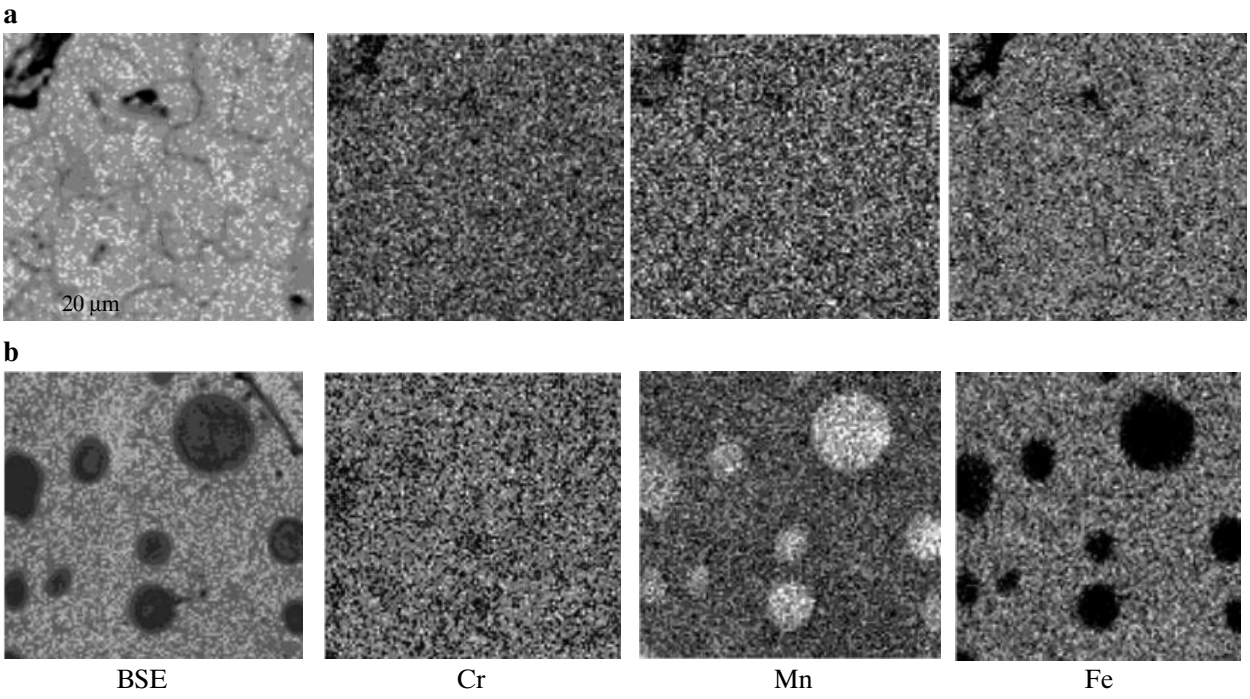

Fig. 4. Back scattered electron image (BSE) and distribution of characteristic X-ray radiation for Fe, Cr and Mn on the surface of 10Cr12Mn20W steel: a – original surface; b – after 3 ion and hydrogen plasma pulses in the PF-1000 device.

the formation of craters or being trapped in the solid state. Manganese from the retained gas phase, as well as compounds of carbon and oxygen condensed onto the inner surface of the bubbles. That is why an increase of manganese, as well as carbon and oxygen content in the vicinity of blisters and craters was observed on the surface of the irradiated steels.

These results show new possibilities of the application of DPF devices for ion-plasma treatment of materials and creation of modified surface layers with new properties.

Simulation of material damage under plasma disruptions in thermonuclear fusion reactor

In the work [23], we proposed a new experimental technique using the DPF devices where irradiation conditions in the cathode part of PF chamber would be similar to plasma disruption regime in the thermonuclear fusion reactor with magnetic confinement of the plasma. In accordance with this technique, the tested specimen represents an elongated cylinder tube (parameters of the tube presented in chapter "Test specimen"). Irradiation conditions for this case are presented in Table 1. As can be seen from the table the time of interaction between the DP pulse and the tube surface increased about 2 times, while the value q decreases approximately 5 times when the distance $L(A)$ increased from 20 to 36 cm. At the same time the thickness of the melted surface layer d decreased about 3.5 times. Besides, it is evident that application of a protective screen provided a decrease of q by approximately 2–3 orders of magnitude in comparison with the value of $q = 10^9$ W/cm^2 for the screen surface (no protection). The data concerning plasma disruption in the ITER reactor and interaction conditions of the pulsed deuterium plasma with the tube material in our experiment (Table 2) are presented in [23]. Damage factor $F = q \cdot \tau^{0.5}$ in Table 2 is the parameter, which allows comparing the surface damage under different irradiation conditions [23, 24]. From the table, it is seen that the damage factor of the material in our experiments conformed to the one for plasma disruption conditions in ITER within one order of magnitude.

On the basis of experimental results and numerical estimation we suppose that the DPF devices may be applied to simulate thermal conditions of the material

Table 1. Observed parameters of irradiation

Number of the tube specimen	1	2	3	4	5
Distance between the specimen and the anode $L(A)$, cm	20	24	28	32	36
Duration of interaction between the specimen and the plasma stream τ, μs	1.9	2.4	2.8	3.3	3.9
Thickness of the melted surface layer d, μm	23.8	17.9	12.6	11.2	7.1
Power density of the plasma stream q, 10^6 W/cm^2	5.0	2.5	1.6	1.2	0.8

Table 2. Possibility to imitate a plasma disruption in the reactor ITER

Damage factor $F = q \cdot \tau^{0.5}$, $W \cdot cm^{-2} \cdot s^{0.5}$			
Plasma disruption in reactor ITER [8, 17]		Influence of pulsed plasma upon the tube material in PF-1000 device	
The first wall	Divertor plate	The nearest to the anode part	The outermost from the anode part
$\sim(10^3–10^4)$	$\sim(10^3–10^5)$	$\sim 10^4$	$\sim 10^3$

Table 3. Chemical content of the steel tube

	Elements, mass%								
Steel	C	Cr	Mn	Si	W	V	Sc	P	S
25Cr12Mn20W	0.26	12.9	19.3	0.13	2.0	0.15	0.1	0.04	0.008

damage on the first wall and divertor plate of ITER under plasma disruption regime. But approximation of simulation conditions to the conditions of real plasma disruption requires broad experimental research using DPF (μs pulse duration) in comparison with devices of millisecond pulse duration.

Influence of pulsed beams with extreme energy upon the material of low activation austenitic steel tube

The influence of microsecond pulses of deuterium ions and plasma upon the low activation austenitic steel 25Cr12Mn20W tube was investigated in the PF-1000 device. Tubes of this type have a hexagonal shape [25]. Unlike the experiments with a duraluminum tube, the steel tube had no protective screen, so ion and plasma beams irradiated both the external and the internal surface of the tube. The study of material damages, surface relief changes, as well as structure of the re-solidified layer along the external and internal surfaces of the tube was of special interest.

Test specimen

The steel tube was manufactured in the form of a regular hexahedral prism. Formerly, similar hexahedral tubes manufactured from different stainless steels were investigated as covers of heat-generating elements for fission reactors [25]. Tube #14 (25Cr12Mn20W) was selected for our experiments. The length of the tube was $L = 30$ cm, the width of each facet $a = 2.2$ cm and the thickness of the wall $h = 0.1$ cm. The tube was manufactured by rolling. After rolling, the samples were annealed at 1150°C for 10 min. The chemical composition of the steel is presented in Table 3.

Irradiation conditions

The tube was placed along the axis of the PF-1000 device (see Fig. 5). The tube was strongly fixed on two cathode bars by special copper holders. The shortest distance between anode and the tube side was $L_1 \approx 11$ cm. On the opposite cut of the tube the copper arc was fixed. Its dimensions were: arc radius $R \approx 25$ cm, arc length $L \approx 30$ cm, arc width $a \approx 1.5$ cm and arc thickness $h \approx 0.12$ cm. The arc prevented the ion and plasma streams from leaving the tube (see Fig. 5). The energy store in the device PF-1000 was ~ 600 kJ. Pure deuterium at the initial pressure of 470 Pa was used as working gas. Duration τ of the DP pulse moving over the plane of the front cut of the tube was 1 μs. The power density of the plasma beam q at this plane was 10^9 W/cm^2. Power density absorbed by the side surface of the tube was about $\sim 10^6$ W/cm^2. The total number of pulses in our experiments was $N = 4$, and the neutron yield in individual "shots" $n = (10^9 \div 10^{11})$.

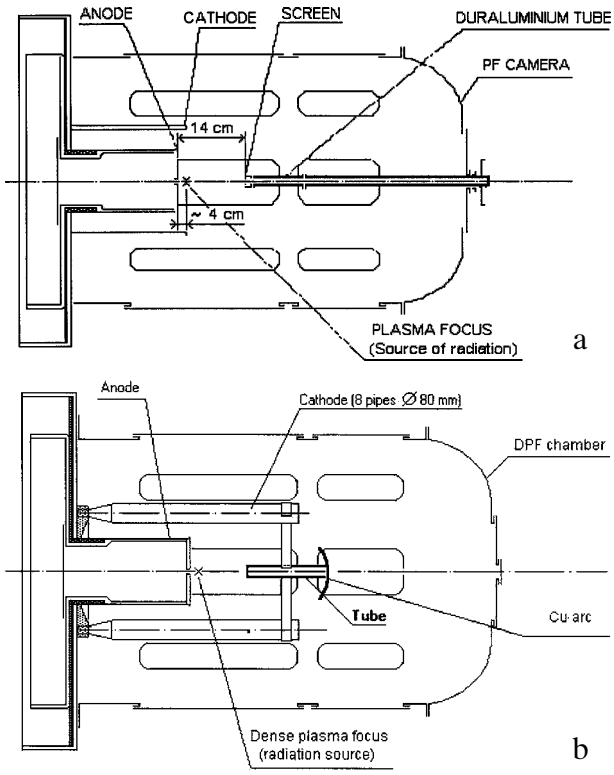

Fig. 5. Scheme of Dense Plasma Focus device PF-1000: a – experiment with a duraluminum tube and protective screen [23, 24]; b – experiment with an hexahedral steel tube.

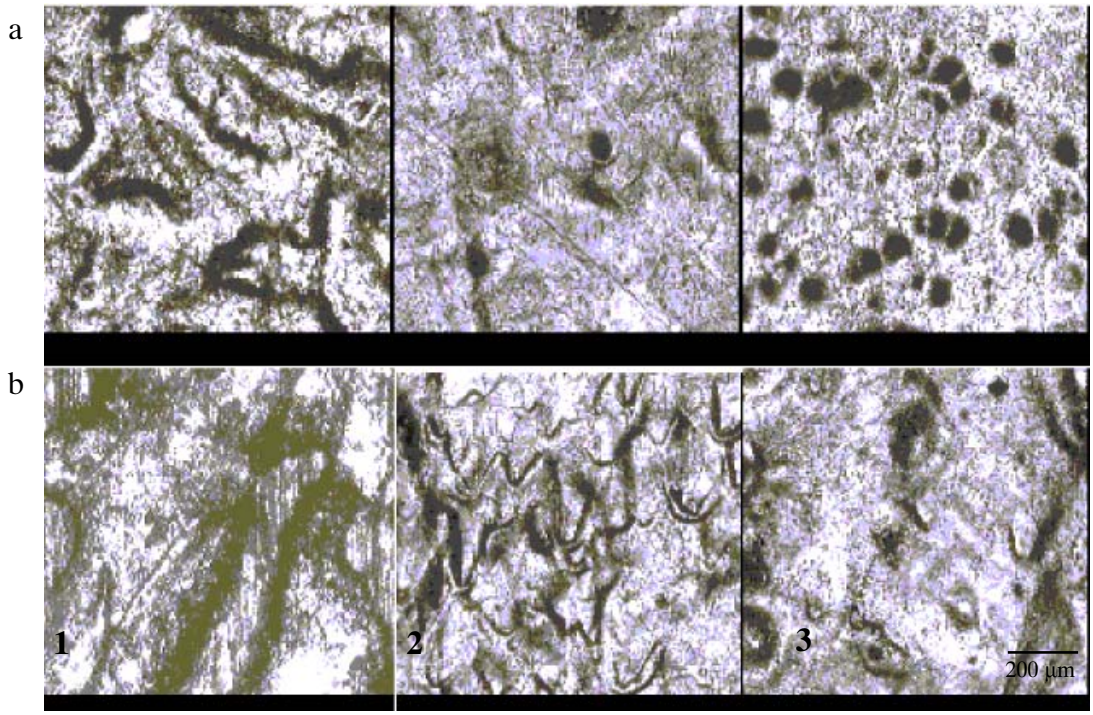

Fig. 6. Parts of the external (a) and internal (b) surfaces of the tube: 1 – in the "hot" zone (specimen #2); 2 – in the middle part (specimen #8); 3 – in the "cold" zone (specimen #14).

Surface relief, microstructure and micro-hardness

Visual analysis showed melting both at the inner and the outer surfaces of the tube. The features of the surface layer damage and micro-relief of irradiated surface are presented in Fig. 6. It is seen that both the inside and outside surfaces have wave-like relief. There are a lot of droplets and ridges; the size of such relief fragments on the inner surface is substantially larger than that on the outer one. With decreasing distance from the irradiation source the typical sizes of the elements of the surface relief get smaller, i.e. the topographic structure of the irradiated surface becomes more dispersed. In other words, the surface relief at the "cold" end of the tube ($q \sim 10^8$–10^9 W/cm^2) is smoother than at the "hot" end ($q \sim 10^6$–10^7 W/cm^2).

The micro-hardness was measured in the re-solidified surface layers, in the areas adjoining to them and in the depth of the samples (in the depth of the tube wall). Figures 7a–7c show that the micro-hardness increases in the zones of outer and inner surface layers. Maximum values H, as a rule, are observed in the surface layers. Hardening of the surface layers is associated with the formation of a specific nonequilibrium microstructure of the steel (see Fig. 8) under ultra-fast quenching of liquid phase (with speed of cooling $\sim 10^8$–10^9 K/s [17]). These results show that the conditions of solidification and structure formations were different in the external and internal surface layers of the tube, as well as in different parts of the tube. Observed re-solidified layer thickness (15–20 μm) requires detailed analysis and temperature estimations. X-ray diffraction analysis showed that the dispersible inclusions of martensite and α-phase were present in the re-solidified surface layers along with the austenite (γ-phase). The volume content of the secondary phases was in the range of 1.5–3.0% in the external surface layer and 5.0–9.5% in the internal one. The dispersion of the secondary phase, as a rule, induce hardening and strengthening of the surface layer. It is obvious that the conditions of pulsed plasma irradiation were essentially different on the external and internal surfaces of the steel tube: in the internal cavity of the tube ions and plasma streams had no opportunity to dissipate within the chamber.

Conclusions

The Plasma Focus devices PF-1000, PF-60, and PF-6 with different gases and different irradiation modes were used to carry out experimental investigations of interactions between pulsed ion and high-temperature plasma beams and on some materials to be applied in structural and functional components of thermonuclear fusion devices with magnetic and inertial plasma confinement, as well as for working chambers of plasma devices.

On the basis of the investigations carried out, a significant progress was achieved in understanding the mechanisms of the influence of high energy nano- and microsecond pulsed beams upon irradiated materials. Particularly, under the different power densities three typical regimes of the influence of ion and plasma beam upon the target material disposed in the cathode part of PF device were found: (i) "implantation" ($q \approx 10^5$–10^7 W/cm^2); (ii) screening of the surface by a secondary plasma cloud ($q \approx 10^7$–10^8 W/cm^2); (iii) absence of implantation ("explosive rupture") ($q \approx 10^8$–10^{10} W/cm^2).

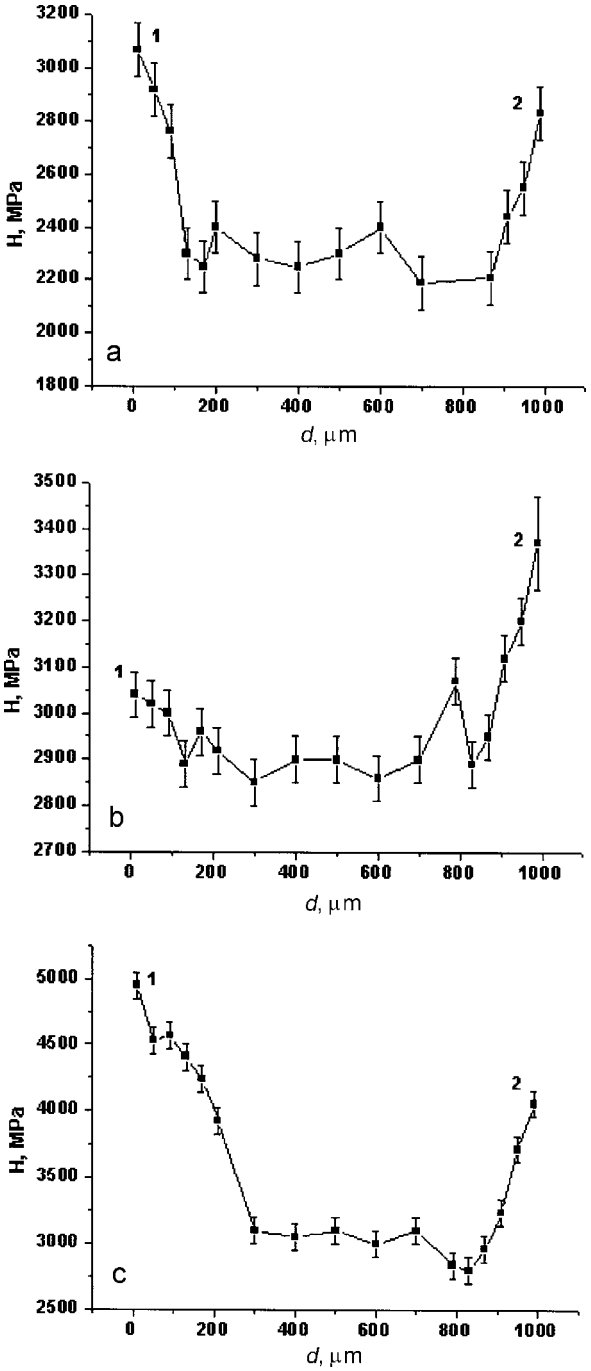

Fig. 7. Distribution of the micro-hardness in the specimens of the irradiated tube in the zone between the external surface layer (1) and the internal one (2): a – sample #1 ("hot"); b – #9 ("middle"); c – #15 ("cold").

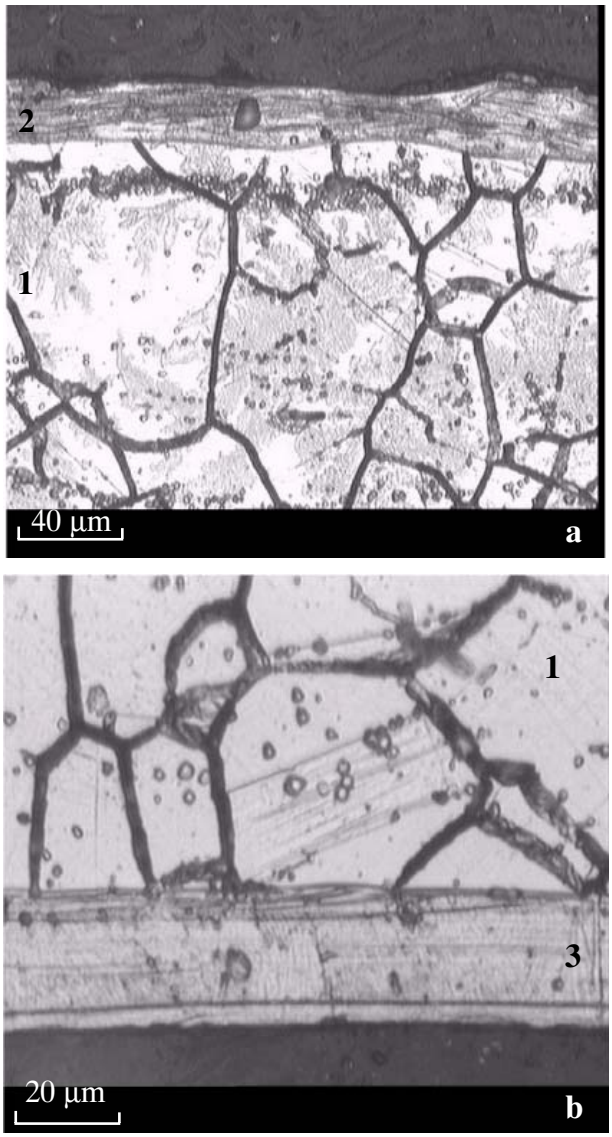

Fig. 8. Cross sections of the steel tube at the central part after irradiation: a – specimen #8; b – specimen #9. 1 – initial microstructure; 2 – remelted layer of the external surface; 3 – remelted layer of the internal surface.

It was shown that the ion and plasma beams in the Dense Plasma Focus devices can be separated temporary and make different energy contribution to the material damage. In this case, the redistribution of the elements in the surface layer of austenitic chromium-manganese steels was found. A remarkable increase of Mn content and a reduction of Fe content took place near the blister-like bubbles formed on the irradiated surface.

The interaction of the pulsed deuterium plasmas and ion beams with the material of an axially oriented tube-like target of the PF-1000 device chamber was studied. Two cases were investigated: with the use of a special protective screen (results were described in [23, 24]) and without it (the low activation steel 25Cr12Mn20W hexahedral tube). In both cases the phase transformation and structure change resulted in hardening and strengthening of the surface layers. These results demonstrated the application possibility of DPF devices to modify the surface layer in hard-to-reach parts of the treated details, such as internal surfaces of the elongated tubes.

Prospects for using the DPF devices to solve scientific and applied problems in material science such as material damage, ion implantation and modification of the surface layers were given. It was also shown that the DPF devices allow to realize the conditions of material damage by high temperature plasma close to that of plasma disruption at ITER. We think that this approach, based on the DPF device application, is very promising to simulate the thermal influence under

plasma disruption at ITER as well as the explosive action of pulsed high-energy beams upon the materials in reactors with inertial confinement of plasma.

Acknowledgment The present work was partially supported by the International Atomic Energy Agency (Research Contracts No.: 11940/R0-R2, 11942/R0-R2, 11943/R0-R2, 12062/R0-R2).

References

1. Abe F, Garner FA, Kayano H (1994) Effect of carbon on irradiation hardening of reduced-activation 10Cr-30Mn austenitic steels. J Nucl Mater 212/215:760–765
2. Borowiecki M, De Chiara P, Gribkov VA *et al.* (2001) Experimental study of a powerful energy flow effect on materials in PF-1000 installation. Nukleonika 46;S1:s117–s122
3. Burtsev VA, Gribkov VA, Filippova TI (1981) High-temperature pinch phenomena. Itogi Nauki i Tekhniki. Fizika Plazmy 2:80–137 (in Russian)
4. Gauster WB, Spears WR and ITER Joint Central Team (1994) Requirements and selection criteria for plasma-facing materials and components in the ITER EDA design. Nucl Fusion 5;Suppl:7–18
5. Gribkov VA, Dubrovsky AV, Miklaszewski R *et al.* (2004) Experimental studies of the ion and plasma beams interaction with carbon-based targets located in the cathode part of Plasma Focus device. In: Proc of the XVIth Int Conf on Physics of Radiation Phenomena and Radiation Material Science, Krym, Alushta, pp 297–298
6. Gribkov VA, Ivanov LI, Maslyaev SA *et al.* (2004) On the nature of changes in the optical characterization produced in sapphire on its irradiation with a pulsed powerful stream of hydrogen ions. Nukleonika 49;2:43–49
7. Gribkov VA, Pimenov VN, Ivanov LI *et al.* (2003) Interaction of high temperature deuterium plasma streams and fast ion beams with condensed materials in Dense Plasma Focus device. J Phys D 36:1817–1825
8. Hassanein A, Konkashbaev I (1994) Erosion of plasma-facing materials during a tokamak disruption. Nucl Fusion 5;Suppl:193–224
9. Ivanov LI, Maslyaev SA, Pimenov VN (1999) The use of liquid metals in porous materials for diverter applications. J Nucl Mater 271/272:405–409
10. Ivanov LI, Pimenov VN, Maslyaev SA *et al.* (2000) Influence of dense deuterium plasma pulses on materials in Plasma Focus device. Nukleonika 45;3:203–207
11. Ivanov LI, Ugaste YE, Pimenov VN, Gribkov VA, Mezzetti F (2000) Mass transport of hydrogen from iron based alloys to outside F environment. Perspektivnye Materialy 2:18–25 (in Russian)
12. Klueh RL, Kenik EA (1994) Thermal stability of manganese-stabilized stainless steels. J Nucl Mater 212/215:437–441
13. Kodentsov AA, Ugaste YE, Pimenov VN *et al.* (2003) Influence of dense deuterium plasma pulses on Fe and Fe-Mn alloy specimens in a plasma focus device. In: Proc of the Tallinn University of Social and Educational Sciences. Tallinn B2:51–56
14. Lawrence Livermore National Laboratory (1992) Inertial confinement fusion. In: 1991 ICF Annual Report, pp 1–198
15. Lyakishev NP, Dyomina EV, Ivanov LI *et al.* (1996) Prospect of development and manufacturing of low activation metallic materials for fusion reactor. J Nucl Mater 233/237:1516–1522
16. Lyublinski IE, Dyomina EV, Evtichin VA *et al.* (1990) Effect of liquid Li on reduced activation Cr-Mn steel. Fizika i Khimiya Obrabotki Materialov 3:131–137 (in Russian)
17. Martynenko YuV, Moskovkin PG, Kolbasov BN (2001) Accumulation and penetration of tritium in the first wall of tokamak ITER in disruption regime. The questions of atomic science and technique. Nucl Fusion 3:65–72
18. Maslyaev SA, Pimenov VN, Platov YM *et al.* (1998) Influence of deuterium plasma pulses generated in plasma focus device on the materials for thermonuclear fusion reactor. Perspektivnye Materialy 3:39–46 (in Russian)
19. Pimenov VN, Dyomina EV, Ivanov LI *et al.* (2002) Damage of structural materials for fusion devices under pulsed ion and high temperature plasma beams. J Nucl Mater 307/311;Part 1:95–99
20. Pimenov VN, Gribkov VA, Dubrovsky AV *et al.* (2002) Influence of powerful pulses of hydrogen plasma upon materials in PF-1000 device. Nukleonika 47;4:155–162
21. Pimenov VN, Gribkov VA, Ivanov LI *et al.* (2003) New possibilities of the application of the Dense Plasma Focus devices to modify material surface layers. Perspektivnye Materialy 1:13–23 (in Russian)
22. Pimenov VN, Gribkov VA, Ivanov LI *et al.* (2004) The pulse influence of extreme energy beams upon low activated austenitic steels. In: Proc of the XVIth Int Conf on Physics of Radiation Phenomena and Radiation Material Science, Krym, Alushta, pp 17–18
23. Pimenov VN, Maslyaev SA, Ivanov LI *et al.* (2003) Interaction of pulsed streams of deuterium plasma with aluminium alloy in a plasma focus device. I. A new methodology of the experiment. In: Proc of the Tallinn University of Social and Educational Sciences. Tallinn B2:30–39
24. Pimenov VN, Maslyaev SA, Ivanov LI *et al.* (2003) Interaction of pulsed streams of deuterium plasma with aluminium alloy in a plasma focus device. II. Investigation of irradiated material. In: Proc of the Tallinn University of Social and Educational Sciences. Tallinn B2:40–50
25. Shamardin VK, Ivanov LI, Demina EV, Bulanova TM, Neustroev VS, Prusakova MD (1989) The influence of neutron beem in the reactor BOR-60 upon the material of the chromium-manganese cover. PHIZHOM 6:5–8 (in Russian)
26. Ugaste YE, Pimenov VN, Ivanov LI *et al.* (2002) Diffusion-stochastic model of the mass transfer of interstitial elements. Calculation of the redistribution of deuterium, implanted in an iron-based alloy. J Adv Mater 9;4:398–405
27. Vertkov AV, Evtichin VA, Lyublinski IE *et al.* (1993) Mechanical properties of low activation Cr-Mn austenitic steel changes in liquid lithium. J Nucl Mater 203:158–163
28. Zabolotnyi VT, Ivanov LI, Suvorov AL (1994) Field-ion microscopy and principal aspects of the radiation damage of the solid. Fizika i Khimiya Obrabotki Materialov 2:5–10 (in Russian)
29. Zabolotnyi VT, Lazorenko VM (1993) Cascades, sub-cascades and peaks of displacement in the tungsten after the irradiation by own ions. Fizika i Khimiya Obrabotki Materialov 3:17–22 (in Russian)